fractal and fractional

MDPI

Article

An Efficient Numerical Method for Pricing Double-Barrier Options on an Underlying Stock Governed by a Fractal Stochastic Process

Samuel Megameno Nuugulu [1,2,*], Frednard Gideon [1] and Kailash C. Patidar [2]

[1] Department of Computing, Mathematical & Statistical Sciences, University of Namibia, Windhoek 13301, Namibia
[2] Department of Mathematics and Applied Mathematics, University of the Western Cape, Bellville 7535, South Africa
* Correspondence: snuugulu@unam.na

Abstract: After the discovery of the fractal structures of financial markets, enormous effort has been dedicated to finding accurate and stable numerical schemes to solve fractional Black-Scholes partial differential equations. This work, therefore, proposes a numerical scheme for pricing double-barrier options, written on an underlying stock whose dynamics are governed by a non-standard fractal stochastic process. The resultant model is time-fractional and is herein referred to as a time-fractional Black-Scholes model. The presence of the time-fractional derivative helps to capture the time-decaying effects of the underlying stock while capturing the globalized change in underlying prices and barriers. In this paper, we present the construction of the proposed scheme, analyse it in terms of its stability and convergence, and present two numerical examples of pricing double knock-in barrier-option problems. The results suggest that the proposed scheme is unconditionally stable and convergent with order $\mathcal{O}(h^2 + k^2)$.

Keywords: time-fractional Black-Scholes PDEs; double barriers options; numerical methods

MSC: 91B24; 91G20; 91G60

Citation: Nuugulu, S.M.; Gideon, F.; Patidar, K.C. An Efficient Numerical Method for Pricing Double-Barrier Options on an Underlying Stock Governed by a Fractal Stochastic Process. *Fractal Fract.* **2023**, *7*, 389. https://doi.org/10.3390/fractalfract7050389

Academic Editor: Leung Lung Chan

Received: 31 January 2023
Revised: 27 March 2023
Accepted: 28 March 2023
Published: 8 May 2023

1. Introduction

Over the years, exotic options have become very popular. Today, a wide variety of exotic options are readily available to investors as they are cheaper, and many offer specific tailor-made protections that have been formulated; see [1–4] and references therein. Several factors can explain the wide popularity of exotic options, one is their almost unlimited flexibility in addressing investors' specific needs, which may not be possible with standard options for which initial formulations are attributed to Black & Scholes [5] the early 70s. Therefore, with exotic options, an investor who would like to hedge against a large drop in an underlying asset price, for example, can sell a down-and-in put option with the barrier set at a lower level as the cheapest way to purchase the underlying asset.

On the other hand, exotic options play a significant hedging role in meeting investors' needs in very cost-effective ways; see for example [1,6,7] and references therein. Rational investors are moving away from buying general protections, and rather focus on designing complex strategies that serve to address their specific exposures at any given point in time. Most of these complex strategies are based on exotic options.

The oldest type of exotic option is the barrier option. Barrier options in general come in two forms—knock-out option (disappearing) or knock-in (appearing), when the underlying asset price triggers some pre-set price levels [8]. Barrier options are thus conditional options, and depend on whether the barrier(s) have been breached during the lifetime of the option.

Barrier options are also part of a class of option called path-dependent. According to Buchen and Konstandatos [1], barrier options are usually cheaper than their vanilla

counterparts. This is due to the fact that a buyer of a barrier option has a more specific view of the underlying asset price dynamics within the time to maturity of the option as compared to its vanilla counterpart. Another hybrid barrier option is the so-called partial-time barrier options [1]. Here, the barrier is monitored (or active) for a time period that is shorter than the expiry time. These options are also called window-barrier options. Another refinement of these kinds of barrier options are those options where barrier(s) are monitored discretely in time. Comprehensive coverage of these kinds of options can be found for example in [8–10] to mention a few.

Another style of barrier options is a double-barrier option, some references to which can be found in [11–14], among others. Under the double-barrier case, there is an upper and a lower barrier. The upper barrier is set above and the lower barrier is below the current underlying asset price. Double knock-in options come to life, and double knock-out options terminate if either of the barriers is hit. It is worth noting that, under double-barrier options, investors can enjoy a greater leverage potential, e.g., under a knock-out option, the barriers can be set too close for comfort, and for knock-ins, the odds of knocking in can also be reduced without much discount [13].

Fractional calculus, and specifically fractional differential equations, are useful mathematical tools for modelling the dynamics of systems and phenomena in very diverse fields in the applied sciences. Some applications can be found in [7,15–20] among others. The discovery of the fractal nature of financial markets, and the subsequent development of fractal-based asset-pricing models, has intensified the search for accurate and stable numerical methods for solving these somewhat involved yet useful asset-pricing models.

Though numerical methods for classical asset-pricing models are abundant, numerical methods for fractional calculus-based models are very much limited. Since fractional models are, to some extent, a generalisation of classical models, several already existing numerical techniques for classical models can be extended to solving fractional ones.

In terms of the Black-Scholes model, there exists a very distinct difference between fractional Black-Scholes and classical Black-Scholes models, in the sense that the derivatives involved in fractional Black-Scholes models are globally defined, while classical models can only capture localized information about a function in a point-wise manner. As such, the non-locality nature of fractional derivatives-based models, among other things, contributes greatly to the complexity of the design, analysis, and implementation of the solution methods for fractional models.

At present, several numerical methods for fractional Black-Scholes models have been suggested. The existing methods can be categorised into three classes: methods based on finite difference [16,19–25], finite elements [26–28] and those based on the spectral approach [29–31]. Compared to the other two classes, the finite difference-based methods are proven to be more robust, efficient and tractable in solving fractional Black-Scholes equations.

In the current work, we extend the concept of double-barrier-option pricing into a time-fractional Black-Scholes framework. Pricing of double-barrier options via the time-fractional Black-Scholes framework is justified by evidence of "long memory" in the time direction observed in many asset time series; see, for example, [32–37]. It is imperative to note that, this desired long decay in the underlying asset in the time direction does not deteriorate the no-arbitrage constraint of asset-pricing theory. For more scientific evidence, see, [19,38,39] and references therein.

The combination of time-fractional Black-Scholes and double-barrier conditions adds additional degrees of complexity in designing solutions to the proposed model. Given the complexity involved, we designed a new robust numerical scheme for solving a time-fractional Black-Scholes model for pricing discrete-monitored double-barrier European options. This paper, therefore, serves to suggest an efficient numerical scheme for solving a time-fractional Black-Scholes model for pricing a discrete double-barrier-option problem.

The rest of this paper is organised as follows. Section 2 presents preliminary concepts and definitions while specifying the model under consideration. Section 3 presents the

detailed construction of the numerical scheme. A comprehensive theoretical analysis of the method in terms of convergence and stability is presented in Section 4. Two practical examples of the use of the approach for pricing double knock-in European put stock options can be found in Section 5. Lastly, Section 6 presents some concluding remarks and sets the scope for future research.

2. Model

This section presents an overview of the preliminary knowledge of the subject of fractional differentiation while specifying the involved tfBS model and its brief derivation background.

2.1. Preliminaries

The most commonly used fractional derivative definitions in modelling financial data are the Caputo, Riemann–Liouville and the Jumarie-revised Riemann–Liouville definition. Though there exist numerous other definitions, these three possess specific properties that make them more appropriate for modelling financial data.

To develop the basis of our model, as well as touch base with the concept of fractional calculus in application to financial modelling and analysis, we will briefly revisit the above three definitions in terms of their mathematical formulations, merits, and demerits.

Definition 1. ***Caputo Derivative***

Let $f : \mathbb{R} \to \mathbb{R}$ be a continuous, but not necessarily a differentiable function. The Caputo fractional derivative of order α is defined as

$$D_t^{\alpha} f(t) = \frac{1}{\Gamma(\eta - \alpha)} \int_0^t \frac{1}{(t-\tau)^{\alpha-\eta+1}} \frac{d^{\eta} f(\tau)}{dt^{\eta}} d\tau, \quad \eta - 1 < \alpha \leq \eta. \tag{1}$$

Though the Caputo fractional derivative of a non-differentiable function may have a kernel at the origin, and that Caputo derivative of a constant function is not zero, according to [19], the Caputo definition allows for the incorporation of traditional initial and boundary conditions into the formulation of the problem, which provides a framework that is consistent with the classical definition.

Definition 2. ***Riemann–Liouville Derivative***

Let $f : \mathbb{R} \to \mathbb{R}$ be a continuous function, but not necessarily differentiable. Then, the Riemann–Liouville fractional derivative of order α is given by

$$D^{\alpha} f(t) = \frac{1}{\Gamma(\eta - \alpha)} \frac{d^{\eta}}{dt^{\eta}} \int_0^t \frac{f(\tau)}{(t-\tau)^{\alpha-\eta+1}} d\tau, \quad \eta - 1 < \alpha \leq \eta. \tag{2}$$

Just as with the Caputo derivative, the Riemann–Liouville derivative of a constant is non-zero, and the derivative of any function that is constant at the origin, for example, the exponential or Mittag–Leffler function, have singularities at the origins. Due to shortcomings in the Caputo and Riemann–Liouville definitions, their applications to modelling several non-linear real-life problems are limited [40].

A modified definition by Jumarie [41] with aid from the definition based on the Generalised Taylor series found in [19,41,42] addresses issues of singularities regarding the origin as well the non-zero constraint of constant functions.

Definition 3. ***Jumarie Derivative***

Let $f : \mathbb{R} \to \mathbb{R}$ be a continuous function, but not necessarily a differentiable, and suppose that $f(t)$ is

(i) a constant K, then its Jumarie fractional derivative of order α is defined by

$$D_t^{\alpha} f(t) = \begin{cases} \frac{K}{\Gamma(\eta-\alpha)} t^{-\alpha+1-\eta}, & \alpha \leq \eta - 1, \\ 0, & \alpha > \eta - 1, \end{cases} \tag{3}$$

(ii) not a constant, then

$$D_t^{\alpha} f(t) = \frac{1}{\Gamma(\eta-\alpha)} \frac{d^{\eta}}{dt^{\eta}} \int_0^t \frac{\{f(\tau)-f(0)\}}{(t-\tau)^{\alpha}} d\tau, \ \ \eta-1<\alpha<\eta, \tag{4}$$

$$D_t^{\alpha} f(t) = \frac{\partial^{\eta} f(t)}{\partial t^{\eta}}, \ \alpha=\eta \tag{5}$$

The Jumarie [37,41,43,44] definition above takes into account the existence of a fractional derivative at the origin, and the existence of a fractional derivative of a constant, therefore aligning the definition consistently well with local derivative-based differential calculus.

2.2. Model Specification

Let S be the stock price that follows the following non-random fractional stochastic process

$$dS = (r-\delta)Sdt + \sigma S\omega(t)(dt)^{\alpha/2}, \ 0<\alpha\leq 1, \tag{6}$$

which is driven by a fractal process $\beta_{\alpha}(t)$ governed by Gaussian white noise $\omega(t)$ such that

$$d\beta_{\alpha}(t) = \omega(t)(dt)^{\alpha/2}. \tag{7}$$

In (6), σ^2 represents the underlying stock volatility and r and δ represents the risk-free interest rate and the continuous dividend yield, respectively.

We note that in the fractional stochastic process (6), the standard Brownian motion is generalised by $\beta_{\alpha}(t)$ defined in (7). Furthermore, when $\alpha=1$, Equation (6) is equivalent to a geometric Brownian motion.

Unlike in the standard Brownian motion, the non-Gaussian fractional process (6) does not make any prior assumptions about the underlying distribution of the stock price (S); see, for example, [20] and references therein. However, (6) does give insights on how the market is scaling with respect to time.

Using (6), we arrive at the time-fractional Black-Scholes (tfBS)-PDE (8) for pricing double-barrier put options, where the fractional derivative is defined in the Caputo sense. Detailed derivations of similar models for pricing standard options can be found in, among others, [19,41,43,44] and references therein.

$$\begin{cases} \frac{\partial^{\alpha} v}{\partial t^{\alpha}} = \left(rv-(r-\delta)\frac{S\partial v}{\partial S}\right)\frac{t^{1-\alpha}}{\Gamma(2-\alpha)} - \frac{\sigma^2\Gamma(1+\alpha)}{2}\frac{S^2\partial^2 v}{\partial S^2}, \ 0<\alpha\leq 1, \\ B_l \leq S \leq B_u, t\in(0,T) \\ v(B_l,t)=R_l, \ V(B_u,t)=R_u. \end{cases} \tag{8}$$

In the above model, (8) B_l and B_u represent the lower and upper knock-in barriers, with R_l and R_u denoting the respective rebates paid when the corresponding barriers are hit. Moreover, r represents the risk-free interest rate and δ the dividend yield paid by the underlying dividend-paying stock.

To the best of our knowledge, there is a limited amount of literature on the subject of high-order solution schemes for barrier-option pricing time-fractional Black-Scholes PDEs, as the topic is still relatively new and limited to vanilla option problems.

Using variable transform ($\tau = T-t$) time to maturity, (8) can be transformed into the following initial value problem (IVP)

$$\tau^{\alpha-1}(T-\tau)^{1-\alpha}\frac{\partial^{\alpha} v}{\partial \tau^{\alpha}} - \left(\frac{rv}{\Gamma(2-\alpha)} - (r-\delta)S^{\alpha}\frac{\partial^{\alpha} v}{\partial S^{\alpha}}\right)(T-\tau)^{1-\alpha} + \frac{\Gamma(1+\alpha)\sigma^2 S^2}{2}\frac{\partial^2 v}{\partial S^2} = 0,$$

which simplifies to

$$\frac{\partial^\alpha v}{\partial \tau^\alpha} - \left(\frac{rv}{\Gamma(2-\alpha)} - (r-\delta)S\frac{\partial v}{\Gamma(2-\alpha)\partial S}\right)\tau^{1-\alpha} + \frac{\Gamma(1+\alpha)\sigma^2 S^2}{2}\frac{\partial^2 v}{\partial S^2} = 0, \quad 0 < \alpha \leq 1, \tag{9}$$

with initial and boundary conditions

$$\left.\begin{array}{l} S \in (B_l, B_u), \\ \tau \in (T, 0), \\ v(B_l, \tau) = R_l,\ v(B_u, \tau) = R_u. \end{array}\right\} \tag{10}$$

Considering the following change in variables $x = ln(S)$ and $v(x,\tau) = e^{r\tau}v(S,\tau)$ and without loss of notations, after simplification, we obtain

$$\frac{\partial^\alpha v(x,\tau)}{\partial \tau^\alpha} = \left(\frac{rv(x,\tau)}{\Gamma(2-\alpha)} - (r-\delta)x\frac{\partial v(x,\tau)}{\Gamma(2-\alpha)\partial x}\right)\tau^{1-\alpha} - \frac{\Gamma(1+\alpha)\sigma^2 x^2}{2}\frac{\partial^2 v}{\partial S^2}, \quad 0 < \alpha \leq 1, \tag{11}$$

with the following initial and barrier conditions

$$\left.\begin{array}{l} v(x,0) = \max(K - e^x, 0),\ 0 < \tau < T, \\ v(b_l, \tau) = r_l,\ v(b_u, \tau) = r_u,\ \ b_l < x < b_u. \end{array}\right\} \tag{12}$$

3. Numerical Scheme

This section presents the construction of the involved numerical scheme in solving (11), subject to initial and barrier conditions (12).

3.1. Model Discretization

Let L and N be positive integers and define $h = (b_u - b_l)/L$ and $k = T/N$ the space and time step-sizes, respectively. We denote $x_l = b_l + lh;$ for $l = 0, 1, 2, \ldots, L$ and $\tau_n = nk;\ n = 0, 1, 2, \ldots, N$, such that $x_l \in [b_l, b_u]$ and $\tau_n \in [0, T]$. Furthermore, we define $v_l^n = v(x_l, \tau_n)$ as the solution at the grid point $(x_l, \tau_n) = (b_l + lh, nk)$.

3.1.1. Temporal Discretization

Let us define

$$\Delta_t v_l^n = \Delta_t v(x_l, \tau_n) = \frac{v(x_l, \tau_n) - v(x_l, \tau_{n-1})}{k^\alpha} = \frac{v_l^n - v_l^{n-1}}{k^\alpha}, \tag{13}$$

and discretize the time-fractional derivative in (11) at the grid point (x_l, τ_{n+1}) by the following quadrature formula

$$\begin{aligned} \frac{\partial^\alpha v(x_l, \tau_{n+1})}{\partial \tau^\alpha} &= \frac{k^{-\alpha}}{\Gamma(2-\alpha)}\sum_{j=0}^{n}\sigma_j\big(v(x_l, \tau_{n-j+1}) - v(x_l, \tau_{n-j})\big) + \frac{\tau_n^{1-\alpha}}{\Gamma(2-\alpha)}k, \\ &= \frac{1}{\Gamma(2-\alpha)}\sum_{j=0}^{n}\sigma_j\Delta_t v(x_l, t_{n-j+1}) + \mathcal{O}(k^2), \end{aligned} \tag{14}$$

where

$$\sigma_j = (j+1)^{1-\alpha} - j^{1-\alpha},\ j = 0, 1, 2, \cdots, n, \tag{15}$$

such that $1 = \sigma_0 > \sigma_1 > \sigma_2 > \cdots > \to 0$ as $j \to n$.

3.1.2. Spatial Discretization

Let us define

$$\Delta_x v_l^n = \Delta_x v(x_l, \tau_n) = \frac{v(x_{l+1}, \tau_n) - v(x_{l-1}, \tau_n)}{h^2} = \frac{v_{l+1}^n - v_{l-1}^n}{h^2}, \tag{16}$$

$$\Delta_{xx}v_l^n = \Delta_x v(x_l,\tau_n) = \frac{v(x_{l+1},\tau_n) - 2v(x_l,\tau_n) + v(x_{l-1},\tau_n)}{h^2} = \frac{v_{l+1}^n - 2v_l^n + v_{l-1}^n}{h^2}. \quad (17)$$

We approximate the spatial derivatives in (11), as follows:

$$\frac{\partial v(x_l,\tau_{n+1})}{\partial x} = \frac{v(x_{l+1},\tau_{n+1}) - v(x_{l-1},\tau_{n+1})}{2h} - \frac{h^2}{6}\frac{\partial^3 v(x_l,\tau_{n+1})}{\partial x^3} + \mathcal{O}(h^4), \quad (18)$$

and

$$\frac{\partial^2 v(x_l,\tau_{n+1})}{\partial x^2} = \frac{v(x_{l+1},\tau_{n+1}) - 2v(x_l,\tau_{n+1}) + v(x_{l-1},\tau_{n+1})}{h^2} - \frac{h^2}{12}\frac{\partial^4 v(x_l,\tau_{n+1})}{\partial x^4} + \mathcal{O}(h^2). \quad (19)$$

3.2. The Full Scheme

To obtain the full numerical scheme, we substitute (14), (18) and (19) into (11) and we obtain the following scheme

$$\begin{aligned} \frac{1}{\Gamma(2-\alpha)}\sum_{j=0}^{n}\sigma_j\Delta_t v_l^{n-j+1} &= \left(rv_l^{n+1} - q\Delta_x v_l^{n+1}\right)\frac{\tau^{1-\alpha}}{\Gamma(2-\alpha)} - \omega(\alpha)\Delta_{xx}v_l^{n+1} - R_l^{n+1} \\ & q = r-\delta,\ n \geq 0,\ \omega(\alpha) = \frac{\Gamma(1+\alpha)\sigma^2 x^2}{2}. \end{aligned} \quad (20)$$

which, after some algebraic manipulations, can be simplified into

$$\sum_{j=1}^{n+1}\varphi_{j-1}v_l^{n-j+1} = av_{l-1}^{n+1} + bv_l^{n+1} + cv_{l+1}^{n+1} + R_l^{n+1} \quad (21)$$

where by

$$\begin{aligned} &a = -k^\alpha q\tfrac{\tau^{1-\alpha}-\omega'}{h^2},\ \ b = k^\alpha\tfrac{\tau^{1-\alpha}r+2\omega'}{h^2},\ \ c = -k^\alpha q\tfrac{\tau^{1-\alpha}-\omega'}{h^2} - 1, \\ &\omega' = k^\alpha\Gamma(2-\alpha)\omega(\alpha),\ \ \varphi_j = \sigma_j - \sigma_{j+1}. \end{aligned}$$

The final scheme is explicitly given by

$$\varphi_0 v_l^n + \cdots + \varphi_{n-1}v_l^1 + \varphi_n v_l^0 = av_{l-1}^{n+1} + bv_l^{n+1} + cv_{l+1}^{n+1}, \quad (22)$$

whereby the left-hand side of the scheme (22) captures the memory effects.

Furthermore, R_l^{n+1} in (21) represents the remainder after truncation, which is given by

$$R_l^{n+1} = \frac{h^2}{12}\left(\frac{\tau^{1-\alpha}}{\Gamma(2-\alpha)}\frac{\partial^3 v_l^{n+1}}{\partial x^3} + \omega(\alpha)\frac{\partial^4 v_l^{n+1}}{\partial x^4}\right) + \mathcal{O}\left(h^2+k^2\right), \quad (23)$$

which implies that,

$$\left|R_l^{n+1}\right| = C\left(h^2,k^2\right), \quad (24)$$

for some constant C independent of h and k. The proof to this result follows in the next section.

4. Theoretical Analysis of the Scheme

In this section, we present the stability and convergence properties of the proposed difference scheme (22).

4.1. Stability Analysis

The stability properties of the proposed scheme (22) will be discussed using the concept of Fourier analysis. Suppose $\hat{v}_l^n$ is an approximate solution to the scheme (22) such that $v_l^n - \hat{v}_l^n = \epsilon_l^n$ for $l = 0, 1, \cdots, L$, then the following theorem holds.

Theorem 1. *The difference scheme in* (22) *is unconditional stable.*

To prove the above theorem, we substitute the roundoff error ϵ_l^n into (22), we obtain

$$\sum_{j=1}^{n+1} \varphi_{j-1}\epsilon_l^{n-j+1} = a\epsilon_{l-1}^{n+1} + b\epsilon_l^{n+1} + c\epsilon_{l+1}^{n+1}, \tag{25}$$

such that $\epsilon_0^n = \epsilon_L^n = 0$.

Let us define the grid function as follows,

$$\epsilon^n(x) = \begin{cases} \epsilon_l^n, & \text{when } x_l - \frac{h}{2} < x \le x_l + \frac{h}{2}, \ l = 1, 2, \ldots, L-1, \\ 0, & \text{when } b_l \le x \le b_l + \frac{h}{2} \text{ or } b_u - \frac{h}{2} < x \le b_u + \frac{h}{2}, \end{cases} \tag{26}$$

which can be expanded in terms of the following Fourier series representation

$$\epsilon^n(x) = \sum_{j=1}^{\infty} \varrho_n(j) e^{i2\pi jx/b_u - b_l}, \quad n = 1, 2, \ldots, N, \tag{27}$$

where

$$\varrho_n(j) = \frac{1}{b_u - b_l} \int_0^{b_u - b_l} \epsilon^n(x) e^{-i2\pi jx/b_u - b_l} dx, \quad n = 1, 2, \ldots, N, \tag{28}$$

and $i = \sqrt{-1}$.

Let $\epsilon^n = (\epsilon_1^n, \epsilon_2^n, \cdots, \epsilon_{L-1}^n)^T$ and, define its norm

$$\|\epsilon^n\|_2 = \left(\sum_{l=1}^{L-1} h | \epsilon_l^n |^2 \right)^{1/2} = \left(\int_0^{b_u - b_l} | \epsilon^n(x) |^2 dx \right)^{1/2}, \tag{29}$$

and apply the Parseval equality to obtain

$$\int_0^{b_u - b_l} | \epsilon^n(x)^2 | dx = \sum_{j=-\infty}^{\infty} | \varrho_n(j) |^2, \tag{30}$$

to obtain

$$\|\epsilon^n\|_2^2 = \int_0^{b_u - b_l} | \epsilon^n(x) |^2 dx = \sum_{j=-\infty}^{\infty} | \varrho_n(j) |^2 . \tag{31}$$

Therefore, the solution to (25) takes the following form

$$\epsilon_l^n = \varrho_n e^{i\beta lh}, \tag{32}$$

for $\beta := 2\pi j/b_u - b_l$ and $i = \sqrt{-1}$. Substituting the expression for ϵ^n into (25) we obtain

$$\varphi_0\varrho_n e^{i\beta lh} + \cdots + \varphi_{n-1}\varrho_1 e^{i\beta lh} + \varphi_n\varrho_0 e^{i\beta lh} = a\varrho_{n+1}e^{i\beta(l-1)h} + b\varrho_{n+1}e^{i\beta lh} + c\varrho_{n+1}e^{i\beta(l+1)h}, \tag{33}$$

Which, after simplifications, leads to

$$(\varphi_0\varrho_n + \cdots + \varphi_{n-1}\varrho_1 + \varphi_n\varrho_0)e^{i\beta lh} = e^{i\beta lh}\varrho_{n+1}\left(ae^{-i\beta h} + ce^{i\beta h} + b\right), \tag{34}$$

$$\varphi_0\varrho_n + \cdots + \varphi_{n-1}\varrho_1 + \varphi_n\varrho_0 = \varrho_{n+1}\left(a\left(e^{-i\beta h} + e^{i\beta h}\right) + b - 1\right), \tag{35}$$

since $\beta_0 = 1$ and $a = c - \beta_0$.

From the Fourier series representation of $\cos \beta h$, we obtain

$$\varphi_0\varrho_n + \cdots + \varphi_{n-1}\varrho_1 + \varphi_n\varrho_0 = \varrho_{n+1}(a\cos\beta h + b - 1). \tag{36}$$

Proposition 1. *Suppose* ϱ_{n+1} *satisfies* (36)*, then* $|\varrho_{n+1}| \le |\varrho_0|$*, for all* $n = 0, 1, 2, \cdots, N$.

Let $n = 0$, then from (36) we have

$$|\varrho_1(a\cos\beta h + b - 1)| \quad = \quad |\varphi_0\varrho_0|, \tag{37}$$

which imply that

$$\begin{aligned} |\varrho_1| &= \left|\frac{\varphi_0\varrho_0}{a\cos\beta h + b - 1}\right|, \\ &\leq \frac{\varphi_0}{|a\cos\beta h + b - 1|}|\varrho_0|, \\ &\leq \frac{1-\beta_1}{|a\cos\beta h + b - 1|}|\varrho_0|, \\ &< \frac{1}{|a\cos\beta h + b - 1|}|\varrho_0|, \ (\because 1-\beta_1 < 1), \\ &< |\varrho_0|, \ \left(\because \frac{1}{|a\cos\beta h + b - 1|} < 1\right). \end{aligned} \tag{38}$$

This implies that,

$$|\varrho_1| \leq |\varrho_0|.$$

For $n = 1$, we suppose $|\varrho_n| \leq |\varrho_0|$ for all $n = 1, 2, \cdots, N$, and show that the same is true for $|\varrho_{n+1}| \leq |\varrho_0|$ for all n.

Proof.

$$\begin{aligned} |\varrho_{n+1}| &= \left|\frac{\sum_{j=1}^{n+1}\varphi_{j-1}\varrho_{n-j+1}}{a\cos\beta h + b - 1}\right|, \\ &\leq \frac{1}{|a\cos\beta h + b - 1|}\sum_{j=1}^{n+1}|\varphi_{j-1}\varrho_{n-j+1}|, \\ &\leq \sum_{j=1}^{n+1}|\varphi_{j-1}\varrho_{n-j+1}|, \left(\because \frac{1}{|a\cos\beta h + b - 1|}\right) < 1, \\ &= \varphi_0|\varrho_n| + \varphi_1|\varrho_{n-1}| + \cdots + \varphi_{n-1}|\varrho_1| + \varphi_n|\varrho_0|, \\ &\leq \varphi_0|\varrho_0| + \varphi_1|\varrho_0| + \cdots + \varphi_{n-1}|\varrho_0| + \varphi_n|\varrho_0|, \\ &= (\varphi_0 + \varphi_1 + \cdots + \varphi_{n-1} + \varphi_n)|\varrho_0|, \\ &= \sum_{j=1}^{n+1}\varphi_{j-1}|\varrho_0|, \\ &= |\varrho_0|, \ \left(\because \sum_{j=1}^{n+1}\varphi_{j-1} = 1\right). \end{aligned} \tag{39}$$

Therefore, $\left\|\epsilon_l^{n+1}\right\|_2 \leq \left\|\epsilon_l^0\right\|_2$, which concludes the proof for Theorem 1. □

4.2. Convergence of the Numerical Scheme

In this subsection, we prove that the proposed scheme (22) converges with temporal order of two and is spatially accurate with fourth order. The analysis will follow the concept of Fourier analysis. Let R_l^{n+1} denote the truncation error involved in the approximation at grid point (x_l, τ_{n+1}), then, from (23), we obtain the following theorem:

Theorem 2. *The difference scheme* (22) *is convergent and converges with order* $\mathcal{O}(k^2 + h^4)$.

Let $\xi_l^n = v(x_l, t_n) - v_l^n$ denote the approximation error at grid point (t_n, x_l), such that $\xi_L^n = 0$, for $n = 1, 2, \cdots, N$ and $\xi_l^0 = 0$, for $l = 0, 1, \cdots, L$. By substituting ξ_l^n into the scheme (22) we obtain

$$\sum_{j=1}^{n+1} \varphi_{j-1}\xi_l^{n-j+1} + R_l^{n+1} \quad = \quad a\xi_{l-1}^{n+1} + b\xi_l^{n+1} + c\xi_{l+1}^{n+1}, \tag{40}$$

Similar to stability analysis, we define the following grid functions

$$\xi^n(S) = \begin{cases} \xi_l^n, & \text{when} \quad x_l - \frac{h}{2} < x \leq S_l + \frac{h}{2}, \quad l = 1, 2, \ldots, L-1, \\ 0, & \text{when} \quad 0 \leq x < \frac{h}{2} \quad \text{or} \quad x_{max} - \frac{h}{2} < S \leq x_{max} + \frac{h}{2}, \end{cases} \tag{41}$$

$$R^n(x) = \begin{cases} C_l^n, & \text{when} \quad x_l - \frac{h}{2} < x \leq x_l + \frac{h}{2}, \quad l = 1, 2, \ldots, L-1, \\ 0, & \text{when} \quad 0 \leq x < \frac{h}{2} \quad \text{or} \quad x_{max} - \frac{h}{2} < x \leq x_{max} + \frac{h}{2}, \end{cases} \tag{42}$$

which implies $\xi^n(x)$ and C_l^n have the following Fourier series representations

$$\xi^n(x) = \sum_{j=1}^{\infty} \tau_n(j) e^{i2\pi jx/x_{max}}; \quad n = 1, 2, \ldots, N, \tag{43}$$

$$R^n(x) = \sum_{j=1}^{\infty} \nu_n(j) e^{i2\pi jx/x_{max}}; \quad n = 1, 2, \ldots, N, \tag{44}$$

where

$$\tau_n(j) = \frac{1}{x_{max}} \int_0^{xmax} \xi^n(x) e^{-i2\pi jx/x_{max}} dx; \quad n = 1, 2, \ldots, N. \tag{45}$$

$$\nu_n(j) = \frac{1}{x_{max}} \int_0^{xmax} R^n(x) e^{-i2\pi jx/x_{max}} dx; \quad n = 1, 2, \ldots, N. \tag{46}$$

Let $\xi^n = (\xi_1^n, \xi_2^n, \cdots, \xi_{L-1}^n)^T$ and $R^n = (R_1^n, R_2^n, \cdots, R_{L-1}^n)^T$, and let us define their norms as follows:

$$\left\| \xi^n \right\|_2 = \left(\sum_{l=1}^{L-1} h | \xi_l^n |^2 \right)^{1/2} = \left(\int_0^{x_{max}} | \xi^n(x) |^2 dx \right)^{1/2}, \tag{47}$$

$$\left\| R^n \right\|_2 = \left(\sum_{l=1}^{L-1} h | R_l^n |^2 \right)^{1/2} = \left(\int_0^{x_{max}} | R^n(x) |^2 dx \right)^{1/2}, \tag{48}$$

and, apply the following Parseval equalities

$$\int_0^{S_{max}} | \xi^n(S)^2 | dS = \sum_{j=-\infty}^{\infty} | \tau_n(j) |^2; \quad n = 1, 2, \ldots, N \tag{49}$$

$$\int_0^{S_{max}} | R^n(S)^2 | dS = \sum_{j=-\infty}^{\infty} | \nu_n(j) |^2; \quad n = 1, 2, \ldots, N \tag{50}$$

to obtain

$$\left\| \xi^n \right\|_2^2 = \sum_{j=-\infty}^{\infty} | \tau_n(j) |^2; \quad n = 1, 2, \ldots, N. \tag{51}$$

$$\left\| R^n \right\|_2^2 = \sum_{j=-\infty}^{\infty} | \nu_n(j) |^2; \quad n = 1, 2, \ldots, N. \tag{52}$$

Based on this analysis, we can therefore propose that

$$\xi^n = \tau_n e^{i\beta lh} \quad \text{and} \quad R^n = \nu_n e^{i\beta lh}, \tag{53}$$

where $\beta = 2\pi j/S_{max}$ and $i = \sqrt{-1}$. Substituting the expressions in (53) into (40) we obtain

$$\sum_{j=1}^{n+1} \varphi_{j-1}\tau_{n-j+1}e^{i\beta lh} = a\tau_{n+1}e^{i\beta(l-1)h} + b\tau_{n+1}e^{i\beta lh} + c\tau_{n+1}e^{i\beta(l+1)h} - \nu_{n+1}e^{i\beta lh}, \quad (54)$$

which implies

$$\left(\sum_{j=1}^{n+1} \varphi_{j-1}\tau_{n-j+1}\right)e^{i\beta lh} = e^{i\beta lh}\tau_{n+1}\left(\left(ae^{-i\beta h} + ce^{i\beta h} + b\right) - \nu_{n+1}\right) \quad (55)$$

which simplify into

$$\sum_{j=1}^{n+1} \varphi_{j-1}\tau_{n+1-j} = \tau_{n+1}(a\cos\beta h + b - 1) - \nu_{n+1}. \quad (56)$$

Therefore

$$\tau_{n+1} = \frac{\sum_{j=1}^{n+1} \varphi_{j-1}\tau_{n+1-j} + \nu_{n+1}}{(a\cos\beta h + b - 1)}. \quad (57)$$

Proposition 2. *Suppose τ_n for $n = 0, 1, \cdots, N$ is a solution to (57); then, there exists some positive constant C such that $|\tau_n| \leq C|\nu_1|$ for all n.*

Proof. It is trivial to show that for $n = 0$, from (57), we have

$$|\tau_1| = \left|\frac{\varphi_0\tau_0 + \nu_1}{(a\cos\beta h + b - 1)}\right| \leq \nu_1. \quad (58)$$

Suppose $|\tau_n| \leq C_0|\nu_1|$, for $n = 1, 2, \cdots, N$, for some constant C independent of h and k. Then,

$$\begin{aligned}
|\tau_{n+1}| &\leq \left|\frac{\sum_{j=1}^{n+1} \varphi_{j-1}\tau_{n+1-j} + \nu_{n+1}}{(a\cos\beta h + b - 1)}\right|, \\
&\leq \sum_{j=1}^{n+1} \frac{1}{|(a\cos\beta h + b - 1)|}(\sigma_{j-1}|\tau_{n-j+1}| + |\nu_{n+1}|), \\
&\leq \sum_{j=1}^{n+1} C_{j-1}(\sigma_{j-1}|\tau_{n-j+1}| + |\nu_{n+1}|), \\
&\leq \sum_{j=1}^{n+1} \sigma_{j-1}C_{j-1}|\tau_{n-j+1}| + C_{n+1}|\nu_1|, \\
&\leq \sum_{j=1}^{n+1} \sigma_{j-1}C_{j-1}|\nu_1| + C_{n+1}|\nu_1|, \\
&= \sigma_0C_0|\nu_1| + \sigma_1C_1|\nu_1| + \sigma_2C_2|\nu_1| + \cdots + \sigma_nC_n|\nu_1| + C_{n+1}|\nu_1|, \\
&\leq \hat{C}(\sum_{j=1}^{n+1} \sigma_{j-1}|\nu_1| + \nu_1), (\hat{C} = \max_{0\leq j\leq n+1}\{C_j\}) \\
&= \hat{C}(\sum_{j=0}^{n+1} \sigma_j)|\nu_1| \\
&= C|\nu_1|.
\end{aligned} \quad (59)$$

We can therefore conclude that the scheme (22) is convergent, and this completes the proof to Theorem 2. □

5. Numerical Results and Discussions

In this section, we present two numerical examples of the pricing of double-barrier knock-in put-option problems.

Example 1. *Consider Equation (8), subject to conditions (12) for pricing a double knock-in put option with the following parameters:* $K = 80,\ r = 0.05,\ \sigma = 0.01,\ T = 1,\ S_{\max} = 120,\ L = 100,\ N = 50, \delta = 0.025,$ *and* $0.075, \alpha = (0.5,\ 0.7,\ 0.9,\ 1.0),$ *with lower barrier located at* $B_l = 6$ *and upper barrier located at* $B_u = 110.$

To asses the effects of change in some key option parameters on the effectiveness of the approach, as well as, the numerical method herein, we considered a second example with two different sets of dividend yields δ, two different sets of barriers, the same interest rate r, the same strike price K, the same maturity time T and the same set of α values.

Example 2. *Consider Equation (8), subject to conditions (12) for pricing double knock-in put options with the following parameters:* $K = 80,\ r = 0.05,\ \sigma = 0.015,\ T = 1,\ S_{\max} = 120,\ L = 100,\ N = 100, \delta = 0.045$ *and* $0.10, \alpha = (0.5,\ 0.7,\ 0.9,\ 1.0),$ *with lower barrier located at* $B_l = 10$ *and upper barrier located at* $B_u = 130.$

Option maturity payoff curves for the two considered examples (Examples 1 and 2, above) are presented in Figures 1 and 2 below.

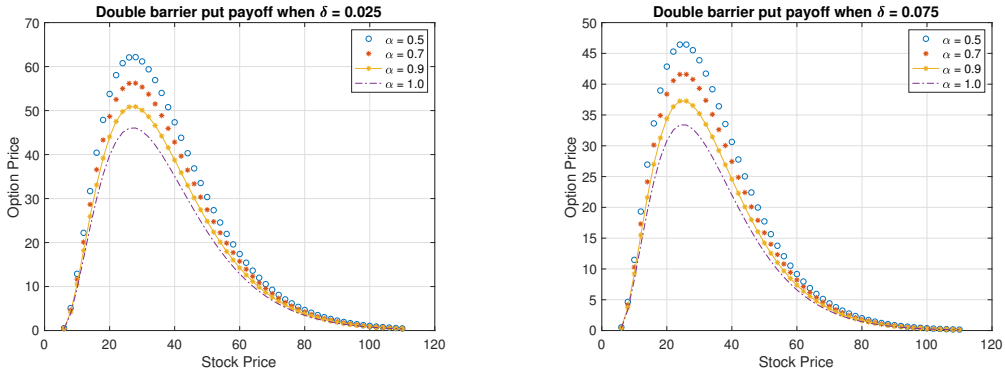

Figure 1. Double-barrier put-option payoffs for $\delta = 0.025,$ and $0.075,$ with $\alpha = (0.5,\ 0.7,\ 0.9,\ 1.0),$ and $B_l = 6,\ B_u = 110$ at $t = T.$

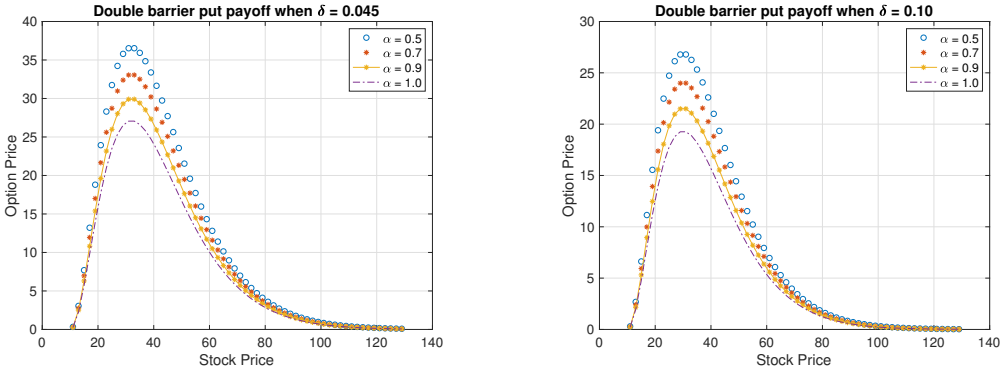

Figure 2. Double-barrier put-option payoffs for $\delta = 0.045,$ and $0.10,$ with $\alpha = (0.5,\ 0.7,\ 0.9,\ 1.0),$ and $B_l = 10,\ B_u = 130$ at $t = T.$

The results in Figures 1 and 2 are consistent with those obtained in [45] which are formulated using a call option. Figures 1 and 2 indicates that, change in dividend yield has an effect on the option price (premium). A higher dividend yield (δ) yields a lower option premium. This is not strange because, the holder of an option with a higher dividend yield

is compensated more through dividends as compared to the one with a lower dividend yield.

Moreover, the considered tfBS in Equation (8) gives high option prices both for the in-the-money option and for when the underlying asset price (S) is close to the strike price (K) as compared to the classical BS model ($\alpha = 1$) case. This indicates that, the tfBS model in (8) is of a *power-law* nature as compared to the classical Black-Scholes model.

Tabular results for the two considered examples (Examples 1 and 2, above) are presented in Tables 1–4, below.

Table 1. Approximation errors for Example 1 with $r = 0.05$ and $\delta = 0.025$.

α	$N = 50$	$N = 100$	$N = 200$	$N = 400$	$N = 800$
0.1	7.1212×10^3	1.7901×10^3	4.4561×10^4	1.1525×10^4	2.9154×10^5
0.2	7.1336×10^3	1.8180×10^3	4.4711×10^4	1.1563×10^4	2.9250×10^5
0.3	7.3465×10^3	1.8383×10^3	4.5753×10^4	1.1827×10^4	2.9717×10^5
0.4	7.4609×10^3	1.9326×10^3	4.8371×10^4	1.2239×10^4	3.0759×10^5
0.5	8.1315×10^3	2.0213×10^3	5.1493×10^4	1.3000×10^4	3.2785×10^5
0.6	8.4515×10^3	2.1032×10^3	5.4620×10^4	1.3842×10^4	3.4915×10^5
0.7	9.5333×10^3	2.3909×10^3	6.1088×10^4	1.5478×10^4	3.7153×10^5
0.8	1.1062×10^2	2.5616×10^3	6.4925×10^4	1.6449×10^4	4.1409×10^5
0.9	1.2494×10^2	3.1452×10^3	7.8208×10^4	2.0062×10^4	5.0548×10^5
1.0	1.3815×10^2	3.4591×10^3	8.7754×10^4	2.2198×10^4	5.5953×10^5

Table 2. Rate of convergence for Example 1 with $r = 0.05$ and $\delta = 0.025$.

α	$N = 100$	$N = 200$	$N = 400$	$N = 800$
0.1	1.91	1.95	1.98	1.99
0.2	1.92	1.96	1.98	1.99
0.3	1.93	1.96	1.98	1.99
0.4	1.93	1.96	1.98	1.99
0.5	1.93	1.97	1.98	1.99
0.6	1.94	1.97	1.98	1.99
0.7	1.94	1.97	1.98	1.99
0.8	1.94	1.97	1.98	1.99
0.9	1.94	1.97	1.98	1.99
1.0	1.94	1.97	1.98	1.99

Table 3. Approximation errors for Example 2 with $r = 0.05$ and $\delta = 0.045$.

α	$N = 100$	$N = 200$	$N = 400$	$N = 800$	$N = 1600$
0.1	6.5512×10^2	1.6492×10^2	4.1892×10^3	1.0597×10^3	2.5953×10^4
0.2	5.7988×10^3	1.4694×10^2	3.7170×10^3	9.4025×10^4	2.3784×10^4
0.3	5.2147×10^2	1.3191×10^2	3.3368×10^3	8.4408×10^4	2.1352×10^4
0.4	4.7443×10^2	1.2001×10^2	3.0358×10^3	7.6794×10^4	1.9426×10^4
0.5	4.3746×10^2	1.1066×10^2	2.7993×10^3	7.0810×10^4	1.7912×10^4
0.6	4.0893×10^2	1.0344×10^2	2.6167×10^3	6.6192×10^4	1.6544×10^4
0.7	3.8773×10^2	9.8080×10^3	2.4898×10^3	6.2752×10^4	1.5688×10^4
0.8	3.7318×10^2	9.4300×10^3	2.3779×10^3	6.0305×10^4	1.4980×10^4
0.9	3.6499×10^2	9.3328×10^3	2.4355×10^3	5.9979×10^4	1.5745×10^4
1.0	3.7328×10^2	9.2895×10^3	2.4246×10^3	5.9803×10^4	1.5670×10^4

Table 4. Rate of convergence for Example 2 with $r = 0.05$ and $\delta = 0.045$.

α	$N = 200$	$N = 400$	$N = 800$	$N = 1600$
0.1	1.95	1.98	1.99	1.99
0.2	1.96	1.98	1.99	1.99
0.3	1.96	1.98	1.99	1.99
0.4	1.96	1.98	1.99	2.00
0.5	1.97	1.98	1.99	2.00
0.6	1.97	1.98	1.99	2.00
0.7	1.97	1.98	1.99	2.00
0.8	1.97	1.98	1.99	2.00
0.9	1.97	1.98	1.99	2.00
1.0	1.97	1.98	1.99	2.00

The numerical results herein confirm our theoretical deductions on the stability and convergence properties of the scheme as presented in Sections 4.1 and 4.2, respectively. The

results indicates that, the proposed scheme is unconditionally stable (see Section 4.1) and converges with order $\mathcal{O}(h^2, k^2)$, i.e., the scheme converges with order two in both time and asset directions under all possible orders of the fractional derivative (α).

6. Concluding Remarks and Scope for Future Direction

In this paper we considered a double-barrier-option pricing problem under the time-fractional Black-Scholes setup. We propose a robust second-order numerical scheme for solving a discretely monitored double-barrier time-fractional Black-Scholes PDE. Two numerical examples are presented. Results indicates that, adding to the already established scientific evidence, the fractional Black-Scholes approach is a very efficient valuation technique for barrier option problems as compared to the usual/classical Black-Scholes approach. The double barrier-option tfBS model in Equation (8) is sensitive to dividend payouts, and allocates lower put premiums to higher dividend yield options. These results are well in line with the theory of no-arbitrage, where investors who are compensated well in dividends would receive prices lower than those of investors with lower dividend yield options. Moreover, the numerical scheme herein proves to be efficient at solving the involved time-fractional Black-Scholes model, though the approach using the general signal produces some asymmetric performances when $0 < \alpha < 0.5$. The approach is only effective when $0.5 \leq \alpha < 1$, and it is for this reason that we only presented results for when $\alpha = (0.5,\ 0.7,\ 0.9,\ 1.0)$. The calibration of the model to real-time market data remains the subject of future research.

Author Contributions: Conceptualization, K.C.P. and S.M.N.; methodology, K.C.P. and S.M.N.; software, K.C.P. and S.M.N.; validation, K.C.P. and S.M.N. and F.G.; formal analysis, S.M.N.; investigation, S.M.N. and K.C.P.; resources, K.C.P. and F.G.; data curation, S.M.N.; writing—original draft preparation, S.M.N.; writing—review and editing, S.M.N., K.C.P., and F.G.; visualization, S.M.N.; supervision, K.C.P. and F.G; project administration, K.C.P.; funding acquisition, K.C.P. All authors have read and agreed to the published version of the manuscript.

Funding: The research of S. M. Nuugulu was supported by the University of Namibia (Staff Development Program) and DAAD (In-country scholarship). Research for K. C. Patidar is supported by South African National Research Foundation, and F. Gideon was supported by the South African National Research Foundation under NRF-KIC grant of K. C. Patidar.

Data Availability Statement: The data that support the findings of this study are available from the corresponding author, [SM Nuugulu], upon reasonable request.

Conflicts of Interest: The authors declare no conflict of interest.

References

1. Buchen, P.; Konstandatos, O. A new approach to pricing double barrier options with arbitrary payoffs and exponential boundaries. *Appl. Math. Financ.* **2009**, *6*, 497–515. [CrossRef]
2. Hull, J. *Options, Futures and Other Derivatives*; Pearson Prentice Hall: Upper Saddle River, NJ, USA, 2009.
3. Luca, V.B.; Graziella, P.; Davide, R. A very efficient approach for pricing barrier options on an underlying described by the mixed fractional Brownian motion. *Chaos Solitons Fractals* **2016**, *87*, 240–248.
4. Wilmott, P. *Derivatives: The Theory and Practice of Financial Engineering*; John Wiley & Sons: West Sussex, UK, 1998.
5. Black, F.; Scholes, M. The pricing of options and corporate liabilities. *J. Polit. Econ.* **1973**, *81*, 637–654. [CrossRef]
6. Ballerster, R.; Company, C.; Jodar, L. An efficient method for option pricing with discrete dividend payment. *Comput. Math. Appl.* **2008**, *56*, 822–835. [CrossRef]
7. Kleinert, H.; Korbel, J. Option pricing beyond Black-Scholes based on double-fractional diffusion. *Phys. A* **2016**, *449*, 200–214. [CrossRef]
8. Broadie, M.; Glasserman, P. A continuity correction for discrete barrier options. *Math. Financ.* **1997**, *4*, 325–348. [CrossRef]
9. Ahn, D.; Gao, B.; Figlewski, S. Pricing discrete barrier options with an adaptive mesh model. *Quant. Anal. Financ. Mark.* **2002**, *33*, 296–313.
10. Feng, L.; Linetsky, V. Pricing discretely monitored barrier options and defaultable bonds in levy process models: A fast Hilbert transform approach. *Math. Financ.* **2008**, *3*, 337–384. [CrossRef]
11. Hsiao, Y.L.; Shen, S.Y.; Wang, A.M.L. Hybrids finite difference method for pricing tow-asst double barrier options. *Math. Probl. Eng.* **2015**, *2015*, 692695. [CrossRef]

12. Jeon, J.; Kim, J.Y.; Park, C. An analytic expansion method for the valuation of double-barrier options under as stochastic volatility model. *Math. Anal. Appl.* **2016**, *449*, 207–227. [CrossRef]
13. Song, S.; Wang, Y. Pricing double barrier options under a volatility regime-switching model with psychological barriers. *Rev. Deriv. Res.* **2017**, *2*, 225–280. [CrossRef]
14. Bollersleva, T.; Gibson, M.; Zhoud, H. Dynamic estimation of volatility risk premia and investor risk aversion from option-implied and realized volatilities. *J. Econom.* **2011**, *160*, 235–245. [CrossRef]
15. Benson, D.A.; Wheatcraft, S.W.; Meershaert, M.M. Application of a fractional advection-dispersion equation. *J. Water Resour. Res.* **2000**, *35*, 1403–1412. [CrossRef]
16. Huang, G.; Huang, Q.; Zhan, H. Evidence of one-dimensional scale-dependent fractional advection-dispersion. *J. Contemp. Hydrol.* **2006**, *85*, 53–71. [CrossRef]
17. Cutland, N.J.; Kopp, P.E.; Willinger, W. Stock price returns and the Joseph effect: A fractional version of the Black-Scholes model. *Semin. Stoch. Anal. Random Fields Appl.* **1995**, *36*, 327–351.
18. Chang-Ming, C.; Fawang, L.; Kevin, B. Finite difference methods and a fourier analysis for the fractional reaction sub diffusion equation. *Appl. Math. Comput.* **2008**, *2*, 754–769.
19. Nuugulu, S.M.; Gideon, F.; Patidar, K.C. A robust numerical solution to a time-fractional Black-Scholes equation. *Adv. Differ. Equ.* **2021**, *2021*, 123. [CrossRef]
20. Nuugulu, S.M.; Gideon, F.; Patidar, K.C. A robust numerical scheme for a time-fractional Black-Scholes partial differential equation describing stock exchange dynamics. *Chaos Solitons Fractals* **2021**, *145*, 110753. [CrossRef]
21. Donny, C.; Song, W. An upwind finite difference method for a nonlinear Black-Scholes equation governing European option valuation under transaction costs. *Appl. Math. Comput.* **2013**, *219*, 8811–8828.
22. Liang, J.; Wang, J.; Zhang, W.; Qiu, W.; Ren, F. Option pricing of a bi-fractional Black-Scholes model with the Hurst exponent H in $[1/2, 1]$. *Appl. Math. Lett.* **2010**, *23*, 859–863. [CrossRef]
23. Meerschaert, M.M.; Tadjeran, C. Finite difference methods for two-dimensional fractional dispersion equation. *J. Comput. Phys.* **2006**, *211*, 249–261. [CrossRef]
24. Murio, D.A. Implicit finite difference approximation for time fractional diffusion equations. *Comput. Math. Appl.* **2008**, *56*, 1138–1145. [CrossRef]
25. Wang, H.; Wang, K.X.; Sircar, T. A direct $\mathcal{O}(N \log^2 N)$ finite difference method for fractional diffusion equations. *J. Comput. Phys.* **2009**, *229*, 8095–8104. [CrossRef]
26. Bu, W.P.; Tang, Y.F.; Yang, J.Y. Galerkin finite element method for two-dimensional Riez space fractional diffusion equations. *J. Comput. Phys.* **2014**, *267*, 26–38. [CrossRef]
27. Ford, N.J.; Xiao, J.Y.; Yan, Y.B. A finite element method for time fractional partial differential equations. *Fract. Calc. Appl. Anal.* **2011**, *14*, 454–474. [CrossRef]
28. Jiang, Y.J.; Ma, J.T. High-order finite element methods for time-fractional partial differential equations. *J. Comput. Math.* **2011**, *235*, 3285–3290. [CrossRef]
29. Canuto, C.; Hussaini, M.Y.; Quarteroni, A.; Zang, T.A. *Spectral Methods: Fundamentals in Single Domains*; Springer: Berlin/Heidelberg, Germany, 2006.
30. Xu, C.; Lin, Y. Finite difference/spactral approximations for the time-fractional diffusion equation. *J. Comput. Phys.* **2007**, *225*, 1533–1552.
31. Doha, E.H.; Bhrawy, A.H.; Ezz-Eldien, S.S. Effecient chebyshev spectral methods for solving multi-term fractional differential equations. *J. Appl. Math. Model.* **2011**, *35*, 5662–5672. [CrossRef]
32. Kristoufek, L.; Vosvrda, M. Measuring capital market efficiency: Long-term memory, fractal dimension and approximate entropy. *Eur. Phys. J. B* **2014**, *87*, 162. [CrossRef]
33. Sensoy, A.; Tabak, B.M. Time-varying long term memory in the European Union stock markets. *Phys. A* **2015**, *436*, 147–158. [CrossRef]
34. Lahmiri, S. Long memory in international financial markets trends and short movements during the 2008 financial crisis based on variational mode decomposition and detrended fluctuation analysis. *Phys. A* **2015**, *437*, 130–138. [CrossRef]
35. Panas, E. Long memory and chaotic models of prices on the London metal exchange. *Resour. Policy* **2001**, *4*, 485–490. [CrossRef]
36. Acharya, V.V.; Richardson, M. Causes of the financial crisis. *Crit. Rev. Found.* **2009**, *21*, 195–210. [CrossRef]
37. Jumarie, G. Merton's model of optimal portfolio in a Black and Scholes market driven by a fractional Brownian motion with short-range dependence. *Insur. Math. Econ.* **2005**, *37*, 585–598. [CrossRef]
38. Garzarelli, F.; Cristelli, M.; Pompa, G.; Zaccaria, A.; Pietronero, L. Memory effects in stock price dynamics: Evidence of technical trading. *Scint. Rep.* **2014**, *4*, 4487. [CrossRef]
39. Chen, W.; Xu, X.; Zhu, S. Analytically pricing double barrier options on a time-fractional Black-Scholes equation. *Comput. Math. Appl.* **2015**, *69*, 1407–1419. [CrossRef]
40. Atangana, A.; Secer, A. A note on fractional order derivatives and table of fractional derivatives of some special functions. *Abstr. Appl. Anal.* **2013**, *2*, 279681. [CrossRef]
41. Jumarie, G. Modified Reimann-Liouville derivative and fractional Taylor series for non-differentiable functions, further results. *Comput. Math. Appl.* **2006**, *51*, 1367–1376. [CrossRef]
42. Osler, T.J. Taylor's series generalized for fractional derivatives and applications. *SAIM-J. Math. Anal.* **1971**, *2*, 37–47. [CrossRef]

43. Jumarie, G. Stock exchange fractional dynamics defined as fractional exponential growth driven by (usual) Gaussian white noise. Application to fractional Black-Scholes equations. *Insur. Math. Econ.* **2008**, *42*, 271–287. [CrossRef]
44. Jumarie, G. Derivation and solutions of some fractional Black-Scholes equations in coarse-grained space and time. Application to Merton's optimal portfolio. *Comput. Math. Appl.* **2010**, *59*, 1142–1164. [CrossRef]
45. Zhang, H.; Liu, F.; Turner, I.; Yang, Q. Numerical solution of the time fractional Black-Scholes model governing European options. *Comput. Math. Appl.* **2016**, *71*, 1772–1783. [CrossRef]